

## Crystal Structure and Isomerism of a Tumour Targeting Radiopharmaceutical: $[\text{ReO}(\text{dmsa})_2]^-$ ( $\text{H}_2\text{dmsa} = \text{meso-2,3-Dimercaptosuccinic Acid}$ )

Jaspal Singh,<sup>a</sup> Anne K. Powell,<sup>b</sup> Susan E. M. Clarke<sup>c</sup> and Philip J. Blower<sup>\*,d</sup>

<sup>a</sup> Biological Laboratory, The University, Canterbury CT2 7NJ, UK

<sup>b</sup> Chemistry Department, University of East Anglia, Norwich, UK

<sup>c</sup> Nuclear Medicine Department, Guy's Hospital, London SE1, UK

<sup>d</sup> Nuclear Medicine Department, Kent and Canterbury Hospital, Canterbury CT1 3NG, UK

A crystal structure determination shows that one isomer of the complex anion  $[\text{ReO}(\text{dmsa})_2]^-$  ( $\text{H}_2\text{dmsa} = \text{meso-2,3-dimercaptosuccinic acid}$ ), a compound which in radiopharmaceutical form has been shown to localise in certain human tumours, has a square-pyramidal structure with all carboxylic acid groups uncoordinated and oriented *endo* relative to the oxo ligand.

Pentavalent technetium-99m- and rhenium-186-dmsa ( $\text{H}_2\text{dmsa} = \text{meso-2,3-dimercaptosuccinic acid}$ ) are, respectively,  $\gamma$  and  $\beta$  emitting radiopharmaceuticals that undergo *in vivo* localisation in some human tumours, especially medullary thyroid carcinoma. The former is of value in diagnostic imaging of this disease<sup>1</sup> while the latter is now being evaluated as a possible radiotherapeutic analogue.<sup>2,3</sup> The nature of the binding to the target at the molecular level is as yet unknown. The technetium-99m complex has been identified as a mixture of isomers, *syn-endo* 1, *anti* 2 and *syn-exo* 3, by comparison of their chromatographic properties with those of a spectroscopically characterised sample of  $[\text{Bu}_4\text{N}][^{99}\text{TcO}(\text{dmsa})_2]$ .<sup>2</sup> Although these isomers are separable by HPLC it has not been possible to identify unambiguously the separate fractions with specific isomers. <sup>1</sup>H NMR spectroscopy readily distinguishes the *syn*-isomers from the *anti*-isomer,<sup>4</sup> but complete assignment requires recourse to X-ray crystallography. We now report the X-ray crystal structure of the *syn-endo*-isomer of the rhenium complex, both as an aid to assignment of the isomerism and to assist in elucidating the nature of the interaction between the complexes and their biological targets.

*syn-endo*- $[\text{NEt}_4][\text{ReO}(\text{dmsa})_2] \cdot 1\frac{1}{2}\text{H}_2\text{O}$  was prepared by heating together ammonium perrhenate, *meso*-dimercaptosuccinic acid and tin(II) chloride in 1:3:2 mole ratio in water at 100 °C for 40 min. X-Ray quality orange prisms were prepared by repeated recrystallisation, from water, of the solid produced by addition of tetraethylammonium bromide to the cooled, filtered reaction solution.<sup>†</sup>

In the crystal the complex anion adopts an approximate square-pyramidal configuration (slightly distorted towards trigonal bipyramidal) as expected from the spectroscopic properties<sup>2</sup> (Fig. 1). The orientation of the carboxylic acid groups is consistent with the <sup>1</sup>H NMR spectrum (see below) and identifies the complex as the *syn-endo*-isomer. The geometry of the coordination sphere is essentially unaffected by the presence of the carboxylic acid substituents, compared to the analogous ethanedithiolate complex.<sup>5</sup> There is no evidence of significant interaction between these groups and the metal centre at the position *trans* to the oxo-ligand, or of

their protons with the oxo-ligand. Comparison with the structure of the related *syn-endo*-technetium complex of the dimethyl ester of dmsa<sup>6</sup> shows little difference in the core geometric parameters. These similarities are consistent with the assumption that  $[\text{ReO}(\text{dmsa})_2]^-$  and  $[\text{TcO}(\text{dmsa})_2]^-$  accumulate in tumour tissue by analogous mechanisms.

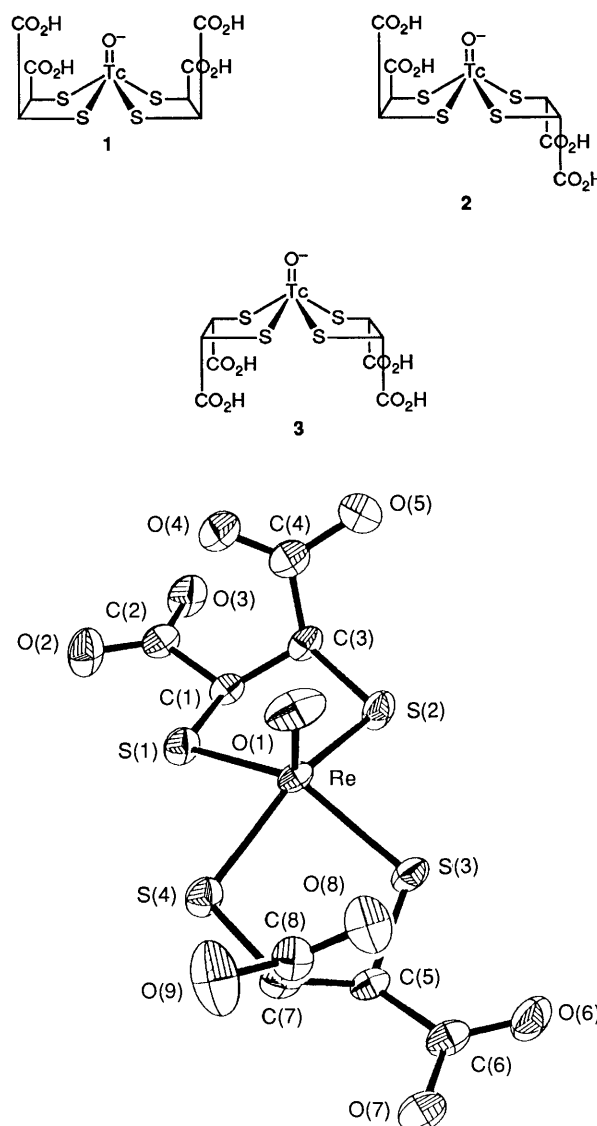


**Fig. 1** Structure of  $[\text{ReO}(\text{dmsa})_2]^-$  (*syn-endo*-isomer). Atoms represented as 50% probability ellipsoids. Selected distances (Å) and angles (°): Re–O(1): 1.699(8); Re–S(1): 2.301(4); Re–S(2): 2.322(4); Re–S(3): 2.286(3); Re–S(4): 2.329(4); O(1)–Re–S(1): 111.2(3); O(1)–Re–S(2): 106.7(4); O(1)–Re–S(3): 113.2(3); O(1)–Re–S(4): 105.3(4).

<sup>†</sup> Crystal data:  $\text{C}_{16}\text{H}_{30}\text{NO}_{10.5}\text{ReS}_4$ ,  $M_r = 718.853$ , triclinic, space group  $P1$ ,  $a = 10.563(4)$ ,  $b = 12.027(5)$ ,  $c = 12.166(3)$  Å,  $\alpha = 106.80(3)$ ,  $\beta = 112.66(3)$ ,  $\gamma = 101.20(3)^\circ$ ,  $V = 1281.1(8)$  Å<sup>3</sup>,  $Z = 2$ ,  $D_c = 1.863$  g cm<sup>-3</sup>, Mo-K $\alpha$  radiation (graphite monochromator),  $\lambda = 0.71073$  Å,  $\mu = 5.169$  mm<sup>-1</sup>,  $F(000) = 712$ , 4141 observed reflections with  $F > 6.0\sigma(F)$ . 4548 independent reflections were collected at 0 °C in an  $\omega - 2\theta$  scan. A semi-empirical absorption correction was applied. The structure was solved (Patterson synthesis) and refined (full-matrix least-squares analysis) using the Siemens SHELXTL PLUS (VMS) system. Refinement converged with  $R = 0.047$ . Carboxylic hydrogens were located from difference maps; the remaining hydrogens were placed at calculated positions. Atomic coordinates, bond lengths and angles, and thermal parameters have been deposited at the Cambridge Crystallographic Data Centre. See Notice to Authors, Issue No. 1.

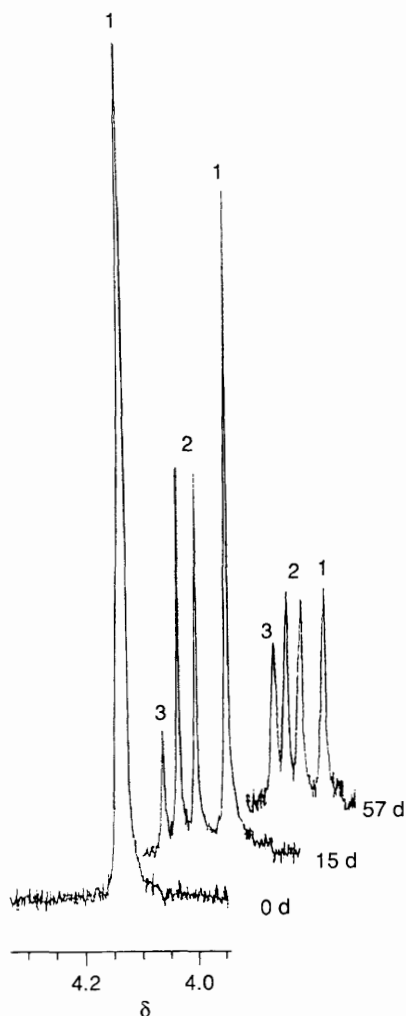


Fig. 2  $^1\text{H}$  NMR spectra of the dmsa C-H region of  $[\text{NET}_4]\text{-}[\text{ReO}(\text{dmsa})_2]$  ( $\text{D}_2\text{O}$  solution, pD 8.7), during incubation for 57 days at room temperature

The intermolecular interactions present in the crystal are of interest in view of their possible relevance to *in vivo* targeting mechanisms. As well as a complex set of intermolecular hydrogen bonding interactions between carboxylic acid groups (in which the water molecules are also involved), there are weak but significant contacts between the rhenyl oxygen atom and two methylene hydrogens of the tetraethylammonium ion to form a loose ring structure with  $\text{O} \cdots \text{H}$  contacts of 2.434 and 2.460 Å. The presence of this interaction suggests that the rhenyl group as well as the carboxylate groups may be capable of a significant hydrogen bonding or dipolar role in target recognition.

Despite the similarity in tumour-targeting behaviour between  $[\text{}^{99\text{m}}\text{TcO}(\text{dmsa})_2]^-$  and  $[\text{}^{186}\text{ReO}(\text{dmsa})_2]^-$ , the rhenium complex shows much greater accumulation in kidney than the technetium analogue.<sup>3</sup> The similarity in the core geometric parameters between rhenium and technetium dithiolate complexes suggests that this difference may be due to differences in non-structural attributes such as kinetics of ligand exchange, the dipole within the  $\text{M}=\text{O}$  bond, or redox behaviour. The group trends in these properties are now being investigated.

In connection with ligand exchange rates, the rate of isomerisation of the complex is of interest. The *syn-endo*- and *anti*-isomers of the rhenium complex undergo pH dependent isomerisation in aqueous solution. This process can be followed by NMR spectroscopy and by HPLC. The  $^1\text{H}$  NMR

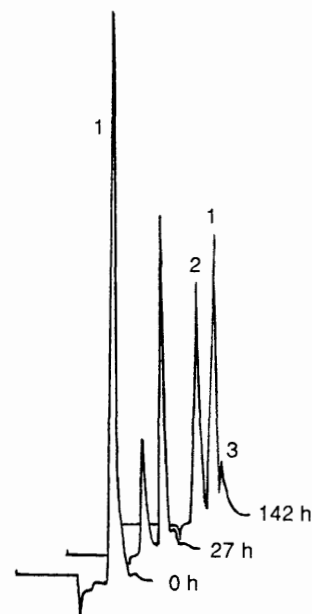


Fig. 3 HPLC of  $[\text{NET}_4][\text{ReO}(\text{dmsa})_2]$  during incubation for 142 h at room temperature at pH 3.9

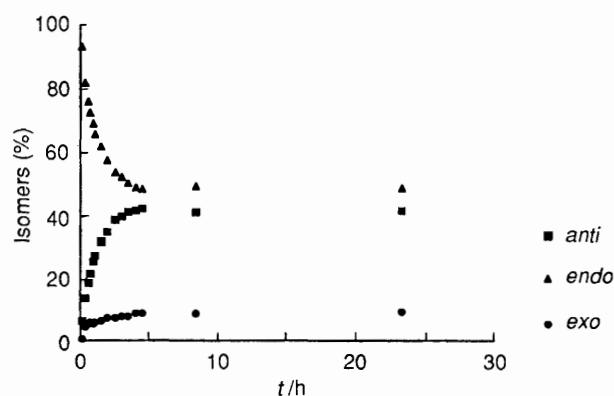


Fig. 4 Isomeric composition of 0.02 molar solution of  $[\text{NET}_4]\text{-}[\text{ReO}(\text{dmsa})_2]$  during incubation at pH 1.5 at room temperature (as determined by HPLC analysis)

spectrum of the sample used for the crystal structure determination (in  $\text{D}_2\text{O}$  containing sodium carbonate, pD ca. 8.7) shows a single resonance at  $\delta$  4.13 corresponding to ligand C-H protons, while the HPLC trace shows a single peak eluting at 7.8 ml.<sup>‡</sup> These properties are consistent with the exclusive presence of the *syn-endo*-isomer identified by the X-ray structure determination. Over a period of several weeks at room temperature the NMR signal decreases in intensity as resonances due to the other two isomers appear ( $\delta$  4.16 and 4.19 corresponding to the *anti*-isomer and  $\delta$  4.23 corresponding to the *syn-exo*-isomer; see Fig. 2). The *anti* isomer is formed faster than the *syn-exo*, consistent with the presumption that the latter is formed *via* the former. These observations correlate with the appearance of two new peaks in the HPLC trace at 6.6 ml (*anti*) and 8.8 ml (*syn-endo*, Fig. 3). There is no significant change in the electronic spectrum during this period, hence the HPLC peak integral at 330 nm is a reliable means of quantitation. Both the rate of isomerisation and the equilibrium isomer distribution are pH dependent.

<sup>‡</sup> HPLC conditions: solvent A: 0.1% trifluoroacetic acid in water; solvent B: 0.1% trifluoroacetic acid in acetonitrile. Gradient (minutes, %B): 0, 0; 5, 40; 6, 40.

dent. At pH 1.5, the half-life of the approach to equilibrium is 3.5 h at room temperature, and the equilibrium composition is 51% *syn-endo*, 40% *anti*, 9% *exo* (see Fig. 4). At pH 3.9 the half-life increases to 23 h, with a similar equilibrium composition. At pH 8.4 the process is very slow and measurements are not complete, but the half-life is several weeks and the equilibrium distribution favours the *syn-exo*-form more strongly (>20% *syn-exo*, >50% *anti*, <30% *syn-endo*). Presumably the major contributor to the relative destabilisation of the *syn-endo*-form at alkaline pH is interligand repulsion between the carboxylate groups, which are all deprotonated at pH 8.4.<sup>4</sup> This repulsion, and that between the carboxylates and the rhenyl oxygen, would be alleviated by isomerisation.

These results suggest that thiolate ligand exchange is acid catalysed, and link structure, NMR spectroscopy and HPLC behaviour in such a way as to allow absolute determination of the isomeric composition of radiopharmaceutical preparations by HPLC alone. This is an essential prerequisite to biological studies aimed at identifying the biodistribution of individual isomers. These results may also help elucidate the molecular interactions involved in binding of the radionuclide within tumour tissue at the cellular and molecular level.

Financial support of this work by the Cancer Research Campaign is gratefully acknowledged. We thank Dr D. O. Smith for obtaining NMR spectra.

Received, 10th June 1991; Com. 1/02786G

## References

- 1 H. Ohta, K. Endo, T. Fujita, J. Konishi, K. Torizuka, K. Horiuchi and A. Yokoyama, *Nucl. Med. Commun.*, 1988, **9**, 105.
- 2 M. M. Bisunadan, P. J. Blower, S. E. M. Clarke, J. Singh and M. J. Went, *Appl. Radiat. Isot.*, 1991, **42**, 167.
- 3 S. J. Allen, G. M. Blake, D. B. McKeeney, C. R. Lazarus, P. J. Blower, J. Singh, C. Page and S. E. M. Clarke, *Eur. J. Nucl. Med.*, 1990, **16**, 432 (abstract).
- 4 P. J. Blower, J. Singh and S. E. M. Clarke, *J. Nucl. Med.*, 1991, **32**, 845.
- 5 P. J. Blower, J. R. Dilworth, J. P. Hutchinson, T. Nicholson and J. Zubieta, *J. Chem. Soc., Dalton Trans.*, 1986, 1339.
- 6 G. Bandoli, M. Nicolini, U. Mazzi, H. Spies and R. Munze, *Transition Met. Chem.*, 1984, **9**, 127.